Limitation and Evaluation of the Two-Broad Standard (TBS) Method of Calibration of Aqueous SEC

S. N. E. OMORODION,* *Chemical Engineering Department, University of Benin, Nigeria,* and A. E. HAMIELEC, *McMaster Institute of Polymer Production Technology, McMaster University, Hamilton, Ontario, Canada L8S 4L7*

Synopsis

Few years ago, the two broad standard method of molecular weight (MW) calibration was proposed[1] and the presence of negative σ^2 (peak dispersion coefficient) was found to be somewhat disturbing. The limitation of the method was not specified. Since large negative values of σ^2 cannot be tolerated, herein is reported another type of instrumental spreading function for which the method may seem to apply, and an evaluation of this method. In its evaluation, plots of $\log_e$ (intercept of a linear molecular weight calibration curve), that is, $\log_e(D_1)$ vs. the corresponding slope of the molecular weight calibration curve, D_2, which were found to be linear, were used. The systems employed were Dextran/Corning controlled porous glass (CPG-10) packing in well-chosen mobile phase.

INTRODUCTION

The two broad molecular weight distribution (MWD) method (TBS) of linear molecular weight calibration is an improved version of both the GPCV2 method of Yau, Stoklosa, and Bly[2] and the effective linear calibration (ELC) method of Balke, Hamielec, et al.[3] When the GPCV2 and ELC methods were stastically evaluated,[4] the ELC method was found to be as good as or better than Yau's modification of it.

The ELC method, which, in principle, assumes no skewing or peak dispersion or Kurtosis effect correction of the experimental chromatogram, is very simple to apply. It is the only method which permits the use of one or two broad MWD standards with the options of using any of the molecular weight averages. The GPCV2 method, which is a modification of the ELC method, accounts for peak dispersion by a method which is somehow questionable. Both methods can only be applied when the instrumental spreading shape function (ISF) is Gaussian in shape. In the TBS method, which uses two standards with known weight and number average molecular weight averages,[1] the ISF was in principle assumed to be Gaussian in shape, since the method was conceived using the analytical solution of Hamielec and Ray[5] of Tung's peak dispersion equation.[6] In view of the fact that negative σ^2 cannot be entertained, the ISF may not only be Gaussian in shape, but in addition, symmetric.

*To whom correspondence should be addressed.

Journal of Applied Polymer Science, Vol. 39, 875–892 (1990)
 CCC 0021-8995/90/040875-18$04.00

In the light of advanced developments which have taken place in the characterization of polymers by SEC in recent years, where the molar mass is now measured directly using on-line detectors such as viscometry, UV and IR spectrophotometry, and low-angle laser light scattering photometry including correction for imperfect resolution, it is important to emphasis the relevancy of the TBS method of molecular weight calibration. To date, no convincing progress has been made trying to:

(i) Establish the true shape of the ISF of each single species in the mass detectors. In many cases, it has always been assumed to be Gaussian in shape. Whether the shape varies for species with the same mean retention volume for complex polymers is yet unknown.[7]

(ii) Find out if peak dispersion coefficient which sometimes is referred to as the axial dispersion coefficient (σ^2) is truly the only measure of peak broadening in SEC under conditions of adequate peak separation. How it is related to the polydispersities of polymers is yet unknown. Usually, the theory used in measuring σ^2 analytically is based on Tung's integral equation which is said to be valid for only monodisperse or very narrow MWD polymers.

(iii) Develop simple analytical methods of estimating σ^2 and ascertaining the true role in σ^2 in SEC, for high MWD polymers, in terms of the influence of flow rate, pore dispersion, polymer/surface area interaction, concentration effect, etc. on σ^2.

(iv) Establish the existence and importance of Kurtosis phenomenon in SEC, since it is known statistically that chromatograms in general can either be thin (leptokurtic) or flat (platykurtic) or remain Gaussian.

(v) Ascertain the fundamental parameters in SEC. It has been established that D_2, which is a measure of peak separation, is fundamentally important. Although the existence of σ^2 is well established, its fundamental relevance is yet unknown. These two parameters are known to be inherent parameters. However, the roles of skewing and kurtosis phenomena are yet to be clearly understood. Skewing of chromatograms can result from improper control of experimental variables such as column overloading, high viscosities, very high flow rates, etc.

The influence of peak dispersion and skewing corrections on the molecular weight calibration curve are to rotate and translate the calibration curves respectively.[3,8-10] When the GPCV2 method was compared with the ELC method, it was observed that "the ELC method calibration line was found to rotate counterclockwisely relative to the peak position calibration line and the extent of rotation was found to increase with increasing dispersion of the column and with decreasing polydispersity" of the polystyrene standards used.[3]

EXPERIMENTAL

The equipment and experimental details have been described already.[11] Dextran standards were used for the following reasons:

(i) As shown in Table I containing the list of the Dextran standards, there are at least eight well-characterized standards as far as provision of both

TABLE I
List of Dextran Standards

Designation	Lot no.	$\bar{M}_n(t) \times 10^{-3}$	$\bar{M}_w(t) \times 10^{-3}$	$\bar{M}_{rms}(t) \times 10^{-3}$	$\bar{M}_w/\bar{M}_n$
T2000	6038	—	—	—	—
T500	5570	173.00	509.00	296.70	2.94
T250	1343	112.50	231.00	161.20	2.05
T150	921	86.00	154.00	115.10	1.79
T110	9071	76.00	106.00	89.80	1.39
T70	1730	42.50	70.00	54.50	1.65
T40	2540	28.90	44.40	35.80	1.54
T20	7968	15.00	22.30	18.29	1.49
T10	3205	5.70	9.30	7.28	1.63

weight average ($\bar{M}_w$) and number average ($\bar{M}_n$) molecular weight are concerned. They cover a wide range of MWs. With the exception of highest MW standard (T2000), the MWD of these standards are also supplied by the manufacturers.

(ii) Dextrans have been one of the most commonly used and studied water-soluble polymers for aqueous SEC application.

(iii) Dextrans are generally believed to be neutral. However, some authors have long reported the contrary.[12-14]

(iv) Peak dispersion estimation and correction in aqueous SEC are yet to be measured with accuracy and ease. The complete characterization of Dextran in terms of its MWD affords this ease.

(v) Dextrans have been one of the easiest water-soluble polymers to study by SEC, probably because of the weak influence of polymer–surface interaction.

Five systems or case studies were employed and their conditions of operation are described in Table II.

THEORY

A few years ago, the TBS method was proposed.[1] In the work, the limitation of the method was not specified except that the instrumental spreading shape function (ISF) was assumed to be Gaussian in shape. In theory, the method should also apply when the ISF is not only Gaussian, but symmetric in shape.

The Linear Two Broad MWD Standard Method

When the ISF is Gaussian, the analytical solutions of Hamielec and Ray[5] of Tung's peak dispersion equation[6] are given in general by

$$\frac{\bar{M}_K(t)}{\bar{M}_K(\text{app})} = \exp\left[\frac{(3 - 2K)D_2^2\sigma^2}{2}\right] = R\sigma^2 \tag{1}$$

where $K = 1, 2, 3, \cdots$ correspond to number-, weight-, z- $\cdots$ average molecular weights. The subscript t refers to the instrumental spreading corrected or true molecular weight averages. The subscript (app) refers to the SEC or

TABLE II
Description and Operating Conditions for Case Studies for Dextran[a]

Case study	Code no.[b]	Columns combined in series	Length of column (ft)	Flow rate (mL/min)	Concn. of injection (wt %)
1	S4BR[c]	729/700, 700/500/370, 240/120, 120/88 Å	15.58	4.50	0.05
2	S5CR[c]	729/700, 700/500/370, 240/120, 120/88, 88 Å	16.75	4.50	0.05
3	S5ER	729/700, 700/500/370, 370/327, 240/120, 88 Å	18.08	4.50	0.05
4	S5FR[d]	729/700, 700/500/370, 370/327, 240/120, 125 Å	18.41	4.50	0.05
5	S6BR	729, 700, 700/500/370, 370/327, 240/120, 120/88, 88 Å	20.75	4.50	0.05

[a] Mobile phase—0.05*M* KF/0.02 wt % NaN_3/1.0 g/24lit. Tergitol/1.0% CH_3OH (pH = 6.6).

[b] The coded form is used and will be preserved, since it may be used to illustrate other phenomena in SEC. The first letter S stands for series combination. The numbers next to S represent the number of columns combined in series. The letter next to the numbers, identifies the system in question and the last letter, R or C, identifies the order of column arrangement. R is for reversed order. This begins with the largest pore size, followed by the next pore size in the decreasing order down to the smallest pore size, instead of the traditional order of column arrangement which begins with the smallest pore size, the conventional method C.

[c] These systems have MW gaps. The intermediate 370/327 Å pore size column which is present in the other systems is not used for these two systems.

[d] Irregular pore-size column arrangement at the end of the multicolumn combination (i.e., small pore-size end).

uncorrected MW averages. D_2 is the slope of the linear MW calibration curve and σ^2 is the variance of the assumed Gaussian shape of each species given by

$$G(v - y) = \sqrt{\frac{1}{2\pi\sigma^2}} \exp\left[\frac{-(v - y)^2}{2\sigma^2}\right] \tag{2}$$

However, when the ISF is in addition symmetric in shape, the analytical solutions of Hamielec and Ray above do not apply, since more than one parameter will now be required to describe this type of shape function. The analytical solution can be assumed to be of the form

$$\frac{\overline{M}_K(t)}{\overline{M}_K(\text{app})} = \exp\left[\frac{(3 - 2K)D_2^2 X}{2}\right] = R_X \tag{3}$$

where X which has now replaced σ^2 is a function of at least two parameters describing the new shape function of which σ^2 is one of them. R_X, which has now replaced $R\sigma^2$, is the MW resolution correction factor. A simple symmetric case can be obtained from the statistical shape function of Provder and

Rosen,[9] in which in the absence of skewing the analytical solutions are

$$\frac{\overline{M}_K(t)}{\overline{M}_K(\text{app})} = \exp\left\{\left[\frac{-(2K-3)D_2^2\sigma^2}{2}\right] \times \left[\frac{1+(A_4/24)\left[(K-2)^4 D_2^4\sigma^4\right]}{1+(A_4/24)\left[(K-1)^4 D_2^4\sigma^4\right]}\right]\right\} \tag{4}$$

where A_4, the second parameter, is the Kurtosis coefficient which could be zero (Gaussian), less than zero (platykurtic), or greater than zero (leptokurtic). A_4 is given by

$$A_4 = \frac{\mu_4}{(\sigma^2)^2} - 3 \tag{5}$$

where μ_4 is the fourth-order moment about the mean retention volume μ_1 of the observed SEC chromatogram. Equation (4) is one of the special cases of eq. (3).

In the TBS method, both the MW calibration curve and the combined ISF or peak broadening parameter X are obtained simultaneously. The equations to be solved, given two broad MWD standards A and B with known $\overline{M}_w(t)$ and $\overline{M}_n(t)$ are therefore given by

$$\overline{M}_n(t_A)\exp\left(\frac{-D_2^2X_A}{2}\right) = D_1\left[\int_0^\infty F_A(v)\exp(D_2\cdot v)\,dv\right]^{-1} \tag{6}$$

$$\overline{M}_n(t_B)\exp\left[\frac{-D_2^2X_B}{2}\right] = D_1\left[\int_0^\infty F_B(v)\exp(D_2\cdot v)\,dv\right]^{-1} \tag{7}$$

$$\overline{M}_w(t_A)\exp\left[\frac{D_2^2X_A}{2}\right] = D_1\left[\int_0^\infty F_A(v)\exp(-D_2\cdot v)\,dv\right] \tag{8}$$

$$\overline{M}_w(t_B)\exp\left[\frac{D_2^2X_B}{2}\right] = D_1\left[\int_0^\infty F_B(v)\exp(-D_2\cdot v)\,dv\right] \tag{9}$$

From these equations,

$$\overline{M}_n(t_i)\cdot\overline{M}_w(t_i) = D_1^2\left\{\int_0^\infty F_i(v)\exp(-D_2\cdot v)\,dv\right\}\left[\int_0^\infty F_i(v)\exp(D_2\cdot v)\,dv\right]^{-1} \tag{10}$$

where i is either A or B. It is seen that the root mean square average MW, $\overline{M}_{\text{rms}}$, defined as $(\overline{M}_n, \overline{M}_w)^{1/2}$ is independent of the ISF parametric correction factor, except when it is skewed.

Taking the ratios of both standards using eq. (10) yields

$$\frac{\bar{M}_{\text{rms}}(t_A)}{\bar{M}_{\text{rms}}(t_B)} = \frac{\left[\int_0^\infty F_A(v)\exp(-D_2 \cdot v)\,dv\right]^{1/2}\left[\int_0^\infty F_B(v)\exp(D_2 \cdot v)\,dv\right]^{1/2}}{\left[\int_0^\infty F_A(v)\exp(D_2 \cdot v)\,dv\right]^{1/2}\left[\int_0^\infty F_B(v)\exp(-D_2 \cdot v)\,dv\right]^{1/2}} \tag{11}$$

Therefore, a single variable search for D_2 results from this equation, followed by a direct calculation of D_1 using eq. (10) for any of the broad standard. Finally, any of the eqs. (6) or (8) and (7) or (9) can now be used to provide for X_A and X_B for each broad MWD standard or R_X, the molecular weight correction factor.

Evaluation of TBS Method of Calibration

In the absence of skewing, the effect of any form of peak dispersion or Kurtosis correction is to rotate the MW calibration curve about a "fixed point."[3,8,9] If there is indeed a single "fixed point," then a plot of $\log_e D_1$ vs. D_2 should be linear and rotate about the "fixed point," regardless of whatever accepted method of calibration is used to generate D_1's and D_2's. Also, if a method of calibration is capable of generating a "true" MW calibration curve, then the true MW calibration curve should be a single point in the plot of $\ln D_1$ vs. D_2 in the linear region of separation of the SEC system for the polymer in question. Therefore, in the absence of skewing or translation and for any method of linear MW calibration,

$$D_1' = J_1^* \exp(J_2^* \cdot D_2') \tag{12}$$

where J_1^* and J_2^* are the intercept and slope, respectively, of plot of $\ln D_1'$ vs. D_2' and the prime is to emphasize that there are several linear MW calibration curves which are being rotated about a "fixed point," the degree of rotation depending on the level of the incorrectly assumed ISF correction factor, based on σ^2. Substituting eq. (12) into the true linear MW calibration curve, $M(v) = D_1 \exp(-D_2 v)$ assuming $D_1' = D_1$, the following is obtained:

$$M(v) = J_1^* \exp(J_2^* \cdot D_2') \cdot \exp(-D_2 \cdot v) \tag{13}$$

When, also,

$$D_2' = D_2, \text{ the slope of the true MW calibration curve,}$$

$$\begin{aligned} M(v) &= J_1^* \exp(D_2 \cdot J_2^*) \cdot \exp(-D_2 \cdot v) \\ &= J_3^* \exp(-D_2 \cdot v) = D_1 \exp(-D_2 \cdot v) \end{aligned} \tag{14}$$

where

$$J_3^* = J_1^* \exp(D_2 \cdot J_2^*) = D_1 \tag{15}$$

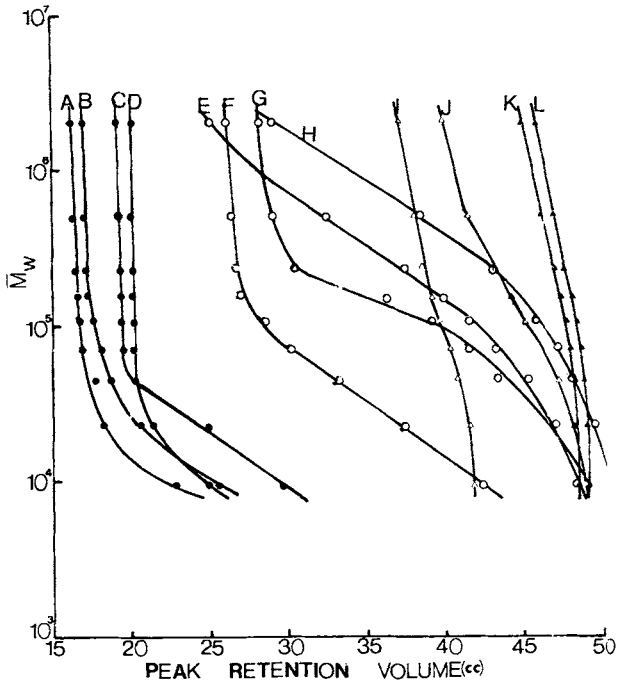

Fig. 1. $\bar{M}_w$ range of separation of different pore sizes for Dextran. Mobile phase = 0.05M KF/0./02 wt % NaN_3/1.0 % CH_3OH/0.04 gm/lit. Tergitol: (A) 88 Å; (B) 120/88 Å; (C) 125 Å; (D) 69 Å; (E) 700/500/370 Å; (F) 240/120 Å; (G) 370/327 Å; (H) 729/700 Å; (I) 2000 Å; (J) 1000 Å; (K) 3000 Å; (L) 3000 Å.

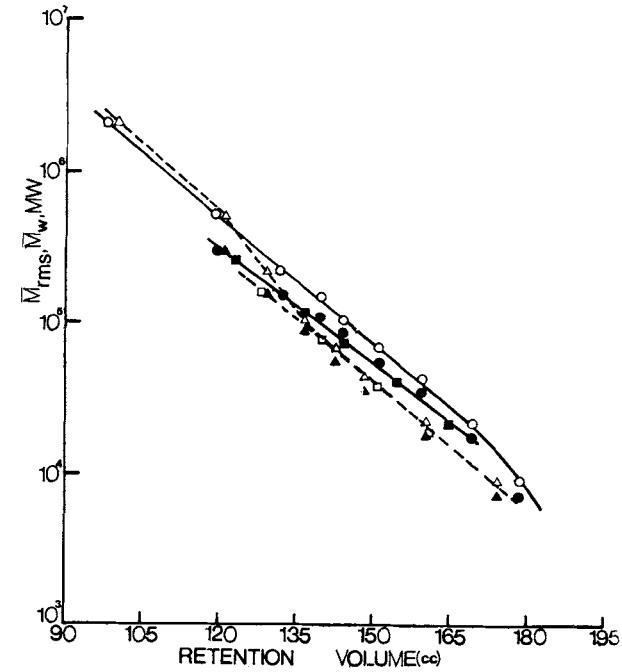

Fig. 2. $\bar{M}_w$, $\bar{M}_{rms}$, and TBS method MW calibration curves for Dextran for case studies # 1 and 2: (○) $\bar{M}_w$, (●) $\bar{M}_{rms}$, (■) TBS method MW calibration curve $M(v) = 0.359 \times 10^9 \exp(-0.300V)$] for case study #1; (△) $\bar{M}_w$, (▲) $\bar{M}_{rms}$, (□) TBS method MW calibration curve $[M(v) = 1.08 \times 10^{-9} \exp(-0.353V)]$ for case study #2.

Therefore, J_3^* is constant. According to eq. (15), the true molecular weight calibration remains the same. Thus, the effect of neglecting corrections of σ^2 parameter associated with X in the absence of skewing is to rotate the MW calibration curves about a "fixed point," the point where the true MW calibration curve lies and where the need for correction does not arise.

RESULTS AND DISCUSSION

Data relevant to the selection of the multicolumn combinations selected for the present studies (Table II) are shown in Figure 1 for single columns of different pore sizes. It is obvious that the large pore sizes 2000 Å and above offer little or no peak separation.[13,14] Where untreated CPG-10 is used as stationary phase for Dextran analysis, addition of salt to the mobile-phase is important.[13,14]

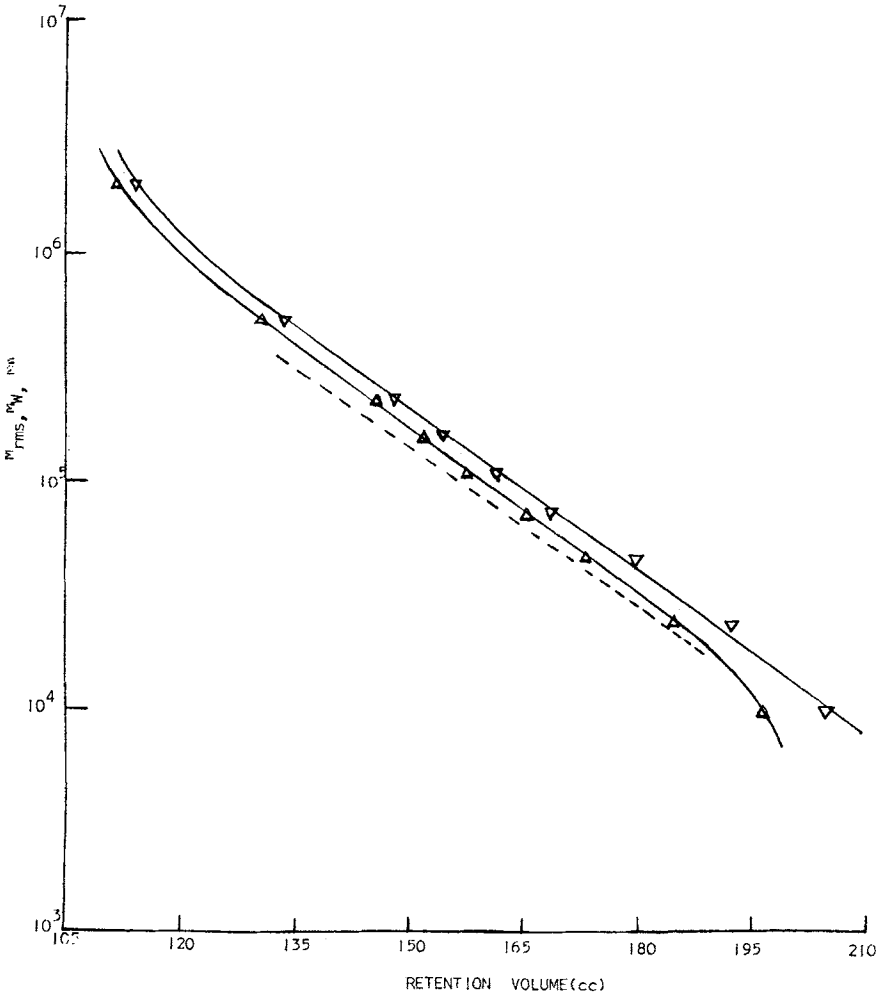

Fig. 3. $\bar{M}_w$ and TBS method MW calibration curves for Dextran for case studies #3 and 4: (△) $\bar{M}_w$ (— · — ·) TBS method MW calibration curve [$M(v) = 0.623 \times 10^9 \exp(0.292V)$] for case study #3; (▽) $\bar{M}_w$, (---) TBS method MW calibration curve [$(M(v) = 0.677 \times 10^9 \exp(-0.286V)$] for case study #4.

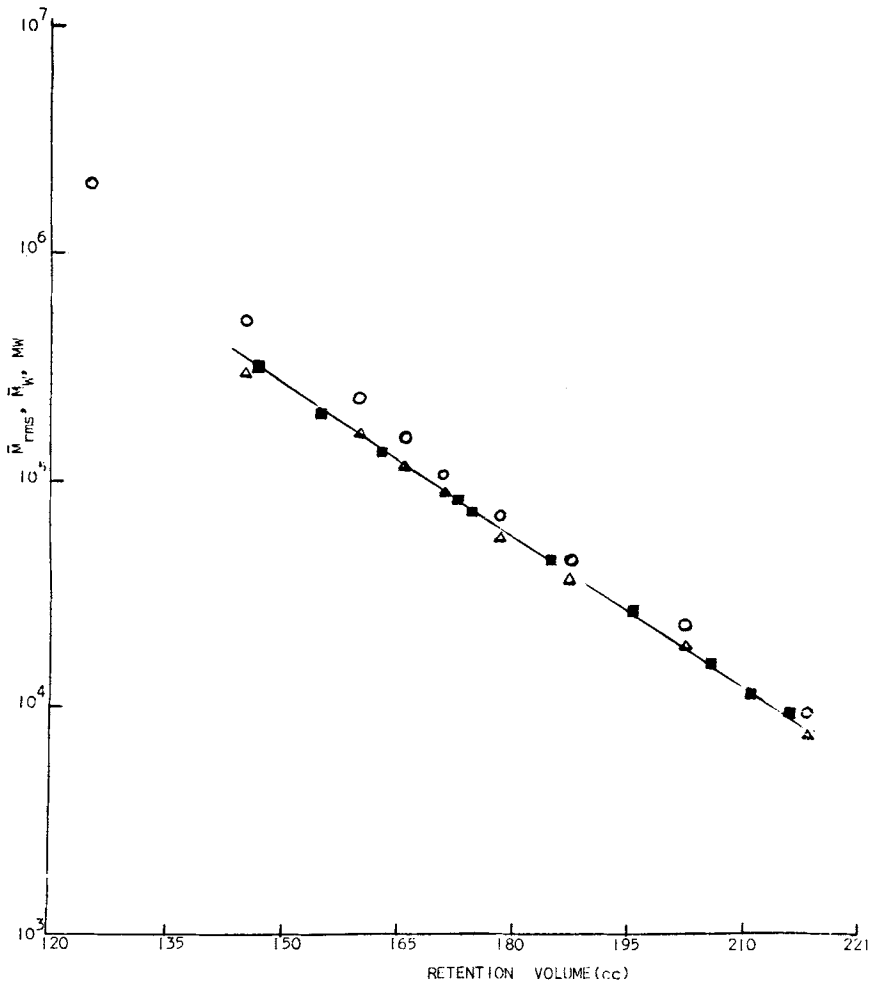

Fig. 4. $\bar{M}_w$, $\bar{M}_{rms}$, and TBS method MW calibration curves for Dextran for case study #5; (○) $\bar{M}_w$, (△) $\bar{M}_{rms}$, (■) TBS method MW calibration curves [$(M(v) = 0.638 \times 10^9 \exp(-0.267V)$].

$\bar{M}_w$ vs. peak retention volumes were first plotted to first ascertain the samples that were within the linear region of the calibration curve. These peak position volume plots (PPV) are shown in Figures 2, 3, and 4 for the coded systems. Using two samples in the linear and/or nonlinear regions one at a time, the TBS method was applied and the results are listed in Table III. X values were also obtained for each pair of samples and these are listed in Table III. Averaging the D_2's and ln D_1's in the linear region of calibration curves, the true MW calibration curves were obtained and these are shown in Figures 2, 3, and 4. In addition, $\bar{M}_{rms}$ versus peak retention volumes were plotted in the figures. Using the true MW calibration curves for each system obtained from the averages of D_2's and D_1's, X values were again obtained for each sample and these are listed in Table IV. Table IV also contains the corresponding R_X values for each sample in each system and those from literature for Dextran. From the table, it is important to note that under the circumstances where the ISF is Gaussian in shape, R_X or $R_{\bar{M}_w}$ values greater

TABLE III
Application of TBS Method—Data for Some Paired Samples of Dextran Standards

	Code no. S5CR					Code no. S5ER				
	Paired samples	X (count)^2	D_1 $\times 10^{-9}$	D_2 (count)$^{-1}$	R_X	Paired samples	X (count)^2	D_1 $\times 10^{-9}$	D_2 (count)$^{-1}$	R_X
			Linear region of calibration					Linear region of calibration		
1	T110	0.099	1.010	0.352	0.994	1 T20	−0.35	0.538	0.289	1.015
	T150	−1.346			1.087	T250	−1.43			1.062
2	T40	0.889	1.730	0.371	0.941	2 T110	0.42	0.497	0.283	0.983
	T250	−0.902			1.064	T500	−5.09			1.226
3	T10	−0.110	1.160	0.357	1.007	3 T150	−0.33	0.737	0.298	1.015
	T110	0.176			0.989	T500	−3.80			1.184
4	T10	−0.120	1.140	0.356	1.008	4 T70	0.86	0.969	0.308	0.960
	T150	−1.225			1.081	T150	0.06			0.997
5	T20	0.151	0.981	0.351	0.991	5 T20	−0.14	0.686	0.295	1.006
	T110	0.081			0.995	T500	−4.03			1.192
6	T20	0.154	0.986	0.351	0.991	6 T40	0.67	0.579	0.289	0.972
	T150	−1.373			1.088	T500	−4.57			1.210
7	T70	0.936	3.79	0.402	0.927	7 T40	0.24	0.394	0.278	0.991
	T250	−0.133			1.011	T250	−2.12			1.085
			Traces of nonlinearity			8 T70	0.29	0.587	0.278	0.988
						T250	−1.25			1.055
	T20	0.410	1.57	0.366	0.973	9 T70	0.69	0.825	0.302	1.021
	T500	−2.953			1.219	T500	−3.47			1.138
	T40	0.970	2.00	0.376	0.934	10 T20	−0.17	0.655	0.294	1.083
	T500	−2.523			1.195	T150	−0.51			1.121
						Traces of nonlinearity				
						T10	−0.68	1.451	0.342	1.036
						T500	−2.00			1.111
						T250	0.39	1.534	0.326	0.980
						T500	−1.87			1.105

TABLE III. (*Continued.*)

	Paired samples	Code no. S4BR X (count)^2	D_1 $\times 10^{-9}$	D_2 (count)$^{-1}$	R_X
1	T40	−0.49	0.317	0.395	1.044
	T250	−0.12			1.034
2	T70	0.22	0.387	0.304	0.990
	T250	−0.04			1.002
3	T40	0.17	0.417	0.301	0.992
	T150	0.01			1.000
4	T110	0.89	0.406	0.304	0.960
	T500	−2.53			1.124
5	T40	−0.06	0.376	0.301	1.003
	T500	−2.77			1.134
6	T40	0.06	0.334	0.297	0.997
	T110	−0.72			1.032
7	T70	−0.37	0.450	0.308	1.018
	T500	−2.21			0.900
8	T150	0.32	0.339	0.296	0.986
	T500	−3.12			0.872
9	T110	−0.61	0.295	0.293	1.026
	T250	0.64			0.973
			Traces of nonlinearity		
	T10	1.08	1.460	0.559	0.845
	T20	1.82			0.753
	T10	−0.65	3.79	0.385	1.049
	T110	2.21			0.849
	T250	0.57	0.553	0.317	0.972
	T500	−1.62			1.085

TABLE III. (*Continued.*)

	Paired samples	Code no. S5FR X (count)^2	D_1 $\times 10^{-9}$	D_2 (count)$^{-1}$	R_X
1	T10	−1.73	0.699	0.291	1.076
	T150	0.18			0.992
2	T20	−0.12	0.808	0.289	1.005
	T500	−1.91			1.083
3	T40	0.88	0.824	0.290	0.964
	T500	−1.85			1.081
4	T10	−1.77	0.670	0.290	1.077
	T250	0.05			0.998
5	T20	−0.19	0.747	0.287	1.008
	T40	0.78			0.968
6	T150	−0.34	0.509	0.280	1.013
	T250	−0.53			1.021
7	T20	−0.61	0.485	0.275	1.023
	T110	0.97			0.964
		Effect of poor pore-size arrangement			
1	T40	−0.01			1.000
	T110	0.70	0.377	0.267	0.975
2	T70	0.16			0.995
	T150	−1.87	0.238	0.255	1.063
3	T20	−1.11			1.039
	T250	−1.76	0.308	0.263	1.063
4	T40	−1.87			1.052
	T70	−1.33	0.116	0.233	1.037
5	T20	−1.06			1.038
	T70	0.67	0.321	0.264	0.977

TABLE III. (*Continued.*)

	Paired sample	Code no. S6BR X (count)^2	D_1 $\times 10^{-9}$	D_2 (count)$^{-1}$	R_X
		Linear region of calibratic	Linear region of calibration		
1	T40	0.75	0.665	0.269	0.973
	T250	−1.56			1.058
2	T20	−0.63	0.621	0.266	1.023
	T150	−1.31			1.048
3	T40	0.80	0.690	0.270	0.972
	T150	−1.12			1.042
4	T150	−1.38	0.598	0.265	1.049
	T250	−1.82			1.066
5	T20	−0.64	0.616	0.266	1.023
	T250	−1.75			1.064
6	T110	0.40	0.462	0.257	0.987
	T250	−2.48			1.086
		Traces of nonlinearity	Traces of nonlinearity		
	T10	0.49	2.687	0.304	0.978
	T20	0.65			0.971
	T10	0.26	1.183	0.284	1.010
	T40	1.39			0.945
	T10	−0.38	1.048	0.282	1.015
	T110	1.24			0.952
	T10	−0.54	0.902	0.278	1.021
	T150	−0.65			1.025
	T10	−0.28	1.165	0.284	1.011
	T500	−3.96			1.173
	T250	1.88	5.091	0.334	1.88
	T500	−0.34			−0.34

TABLE IV
Comparing Calculated R_X Value with Literature Data

Sample	S5CR		S5ER		S5FR		S6BR	
	X[a]	R_X	X	R_X	X	R_X	X	R_X
T10	−0.20	1.013	−1.78	1.079	−1.95	1.083	−1.10	1.040
T20	0.18	0.989	−0.20	1.009	−0.25	1.010	−0.60	1.022
T40	0.55	0.966	0.76	0.968	0.74	0.970	0.66	0.977
T70	0.00	1.000	0.27	0.989	1.70	0.933	0.25	0.991
T110	0.12	0.993	0.65	0.973	1.28	0.948	0.76	0.973
T150	−1.32	1.086	−0.63	1.027	−0.07	1.003	−1.26	1.046
T250	−1.43	1.093	−1.26	1.055	−0.18	1.007	−1.68	1.062
T500	−3.53	1.246	−4.31	1.202	−2.30	1.099	−5.73	1.226

Sample	S4BR		$R_{\bar{M}_w}$[b]	$R_{\bar{M}_w}$[c]	$R_{\bar{M}_w}$[d]	$R_{\bar{M}_w}$[e]
	X	R_X				
T10	−2.76	1.132	1.000	0.830	0.875	1.000
T20	−1.32	1.061	1.018	0.910	0.940	1.115
T40	0.04	0.998	1.047	1.022	0.852	1.057
T70	0.13	0.994	1.103	1.103	—	—
T80	—	—	—	—	1.097	—
T110	0.78	0.966	—	—	1.059	1.050
T150	−0.15	1.007	0.963	0.917	1.196	1.020
T250	−0.12	1.005	0.916	0.889	1.732	1.056
T500	−2.82	1.135	1.028	1.068	2.282	0.974

[a] $(\text{Count})^2$.
[b] Data based on corrected calibration curve for peak dispersion.[15]
[c] Data based on calibration curve obtained iteratively.[15]
[d] Data based on calibration curve obtained by two-step simple iteration.[16]
[e] Data based on peak dispersion corrected calibration curve.[17]

than or equal to 1, which have always been reported in the past, correspond to σ^2 which is negative or zero, respectively. Even for other polymer/SEC systems, the same observations have been reported before.[8,18] Since σ^2 cannot be negative, the assumptions that the ISF is truly Gaussian is questionable. If X is to replace σ^2, for the TBS method to apply, the ISF must in addition be symmetric in shape.

The ELC method was employed for each polymer sample and each system and the results are listed in Table V for four of them. From the data and those of TBS methods, plots of ln D_1 vs. D_2 were obtained and these are shown in Figures 5, 6, and 7. With the exception of S5FR, S5CR, and S4BR, almost single points were obtained in these plots (Figs. 5 and 6) for the TBS method data. System S5FR, which has irregular small pore-size arrangement has the largest variation of D_2, followed by the systems with MW gaps, as shown in Figure 7. It is of interest to note that the plots are linear. It is also of interest to note too that the plots of the data from the ELC method are linear over a wider range of D_2. Each plot is unique to each system. The reason why these plots are linear is not clearly understood. It may be due to the high correlation between D_1 and D_2. However, the search for single points in these plots,

TABLE V
Application of ELC Method of Calibration

Code no. S5CR			Code no. S5FR			Code no. S5ER			Code no. S6BR		
Sample	D_1 $\times 10^{-9}$	D_2 $(\text{count})^{-1}$	Sample	D_1 $\times 10^{-9}$	D_2 $(\text{count})^{-1}$	Sample	D_1 $\times 10^{-9}$	D_2 $(\text{count})^{-1}$	Sample	D_1 $\times 10^{-9}$	D_2 $(\text{count})^{-1}$
				(Single ELC method)							
T10	1.381	0.362	T10	6.490	0.347	T10	3988	0.351	T10	1.543	0.291
T20	0.765	0.343	T20	0.930	0.293	T20	0.805	0.300	T20	1.192	0.283
T40	0.481	0.327	T40	0.379	0.267	T40	0.324	0.272	T40	0.375	0.253
T70	0.938	0.352	T70	0.219	0.252	T70	0.470	0.285	T70	0.494	0.262
T110	0.856	0.345	T110	0.214	0.249	T110	0.332	0.270	T110	0.337	0.247
T150	5.439	0.417	T150	0.623	0.287	T150	0.929	0.306	T150	1.364	0.291
T250	4.432	0.409	T250	0.654	0.289	T250	1.186	0.317	T250	1.421	0.293
T500	15.600	0.463	T500	1.606	0.314	T500	4.030	0.362	T500	6.110	0.340
				(Double ELC method $\overline{M}_n$)							
T10	2.324	0.377	T10	14420	0.423	T10	271.20	0.516	T10	3.022	0.306
T20			T20			T20			T20		
T40	0.121	0.282	T40	0.165	0.244	T40	0.084	0.233	T40	0.085	0.214
T70			T70			T70			T70		
T110	0.014	0.194	T110	0.002	0.105	T110	0.027	0.190	T110	0.008	0.137
T150			T150			T150			T150		
T250	0.227	0.297	T250	8.094	0.369	T500	0.104	0.236	T250	0.302	0.247
T500			T500			T500			T500		
				(Double ELC method $\overline{M}_w$)							
T10	2.936	0.385	T10	6.707	0.348	T10	40.490	0.415	T10	2.367	0.301
T500			T20			T20			T20		
T40	1.902	0.377	T40	0.068	0.227	T40	0.227	0.261	T40	0.212	0.237
T110			T70			T70			T70		
T20	1.662	0.367	T110	0.215	0.249	T110	0.563	0.288	T110	2.024	0.304
T150			T150			T250			T150		
T70	7.695	0.432	T250	56.840	0.461	T150	2.511	0.342	T250	28.720	0.399
T250			T500			T500			T500		

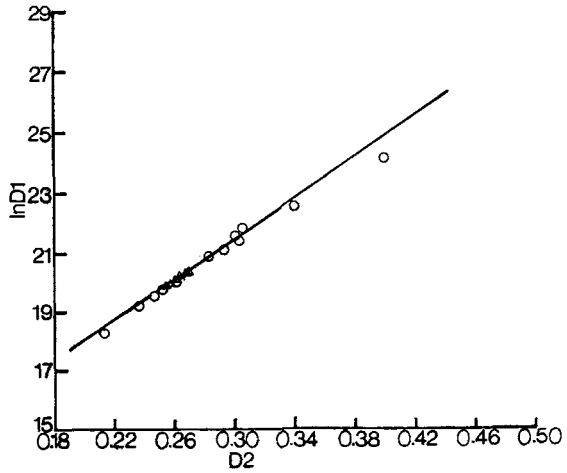

Fig. 5. Evaluation of TBS method for case study #5; (○) based on ELC method; (△) based on TBS method.

the true MW calibration curves, clearly shows the versatility of the TBS method of calibration. In addition, we are able to assess the quality of the system in question.

Finally, as shown in Table VI, which compares J_3^* using eq. (15) with the intercept D_1 of the true MW calibration curves of each system, the excellent agreement shown clearly indicates that there is indeed a linear relationship between ln D_1 and D_2.

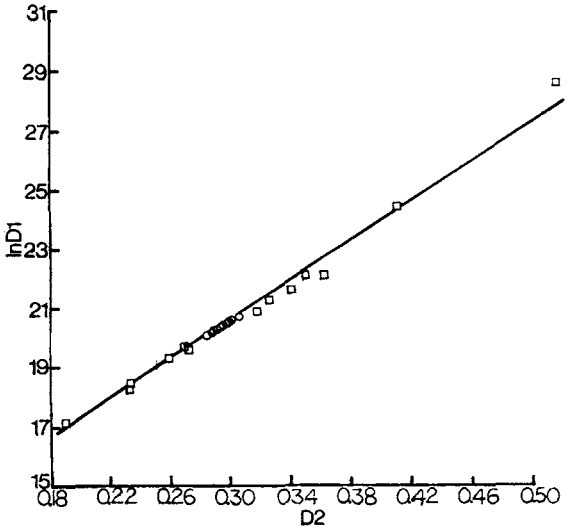

Fig. 6. Evaluation of TBS method for case study #3: (□) based on ELC method; (○) based on TBS method.

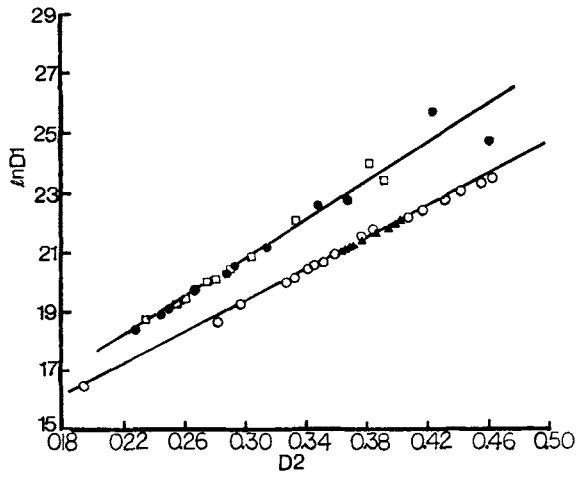

Fig. 7. Evaluation of TBS method for case studies #2 and 4. (●) based on ELC method, (□) based on TBS method for case study #4; (○) based on ELC method, (▲) based on TBS method for case study #2.

TABLE VI
Comparing D_1 with J_3^*

Case study	$J_1^* \times 10^{-5}$	J_2^* (count)	D_2 (count)$^{-1}$	$D_1 \times 10^{-9}$	$J_3^* \times 10^{-9}$
1	0.808	28.00	0.300	0.359	0.359
2	0.935	26.50	0.353	1.080	1.080
3	0.977	30.00	0.292	0.623	0.623
4	0.739	31.87	0.286	0.677	0.672
5	0.926	33.10	0.267	0.638	0.638

CONCLUSION

In summary, it has been shown that the TBS method is a very powerful method in providing a true molecular weight calibration curve. It has also been shown that the method is applicable not only when the analytical solutions of Hamielec and Ray[5] applies, but also when the ISF is in addition symmetric in shape. In the present situation, however, it is difficult to obtain the true MW averages of any sample, using the true MW calibration curve, unless the form of the ISF of each single species is known. The shape of the function will be the subject of the next investigation, subject to which the method will be applied.

References

1. A. E. Hamielec and S. N. E. Omorodion, in *ACS Symposium Series 138*, T. Provder, Ed., Am. Chem. Soc., Washington, DC, 1979, pp. 183–196.

2. W. W. Yau, H. J. Stoklosa, and D. D. Bly, *J. Appl. Polym. Sci.*, **21**, 1911 (1977).

3. S. T. Balke, A. E. Hamielec, B. P. Le Clair, and S. L. Pearce, *Ind. Eng. Chem. Prod. Res. Dev.*, **8**, 54 (1969).

4. M. J. Pollock, J. F. MacGregor, and A. E. Hamielec, *J. Liq. Chromatogr.*, **2**(7), 895 (1979).
5. A. E. Hamielec and W. H. Ray, *J. Appl. Polym. Sci.*, **13**, 1317 (1969).
6. L. H. Tung, *J. Appl. Polym. Sci.*, **10**, 375, 1271 (1966).
7. A. E. Hamielec, *Pure Appl. Chem.*, **54**(2), 293–307 (1982).
8. S. T. Balke and A. E. Hamielec, *J. Appl. Polym. Sci.*, **13**, 1381–1420 (1969).
9. T. Provder and E. M. Rosen, *Sep. Sci.*, **5**(4), 437 (1970).
10. E. M. Rosen and T. Provder, *Sep. Sci.*, **5**(4), 485–521 (1970).
11. S. N. E. Omorodion, A. E. Hamielec and J. L. Brash, in *ACS Symposium Series 138*, T. Provder, Ed., Am. Chem. Soc., Washington, DC, 1979, pp. 267–284.
12. F. A. Buytenhuys and F. P. B. Van Der Maeden, *J. Chromatogr.*, **149**, 489 (1978).
13. S. N. E. Omorodion, A. E. Hamielec, and J. L. Brash, *J. Liq. Chromatogr.*, **4**, 41 (1981).
14. S. N. E. Omorodion, Ph.D. thesis, McMaster University, Canada, 1980.
15. R. R. Vrijbergen, A. A. Soeteman, and J. A. M. Smit, *J. Appl. Polym. Sci.*, **22**, 1267 (1978).
16. K. J. Bombaugh, W. A. Dark, and J. N. Little, *Anal. Chem.*, **41**, 1337 (1969).
17. A. A. Soeteman, J. P. M. Roels, J. A. P. P. Van Dijk, and J. A. M. Smit, *J. Polym. Sci.*, **16**, 2147 (1978).
18. F. L. McCrackin, *J. Appl. Polym. Sci.* **21**, 191–198 (1977).

Received October 31, 1988
Accepted November 3, 1988